Original Research Article, SPECIAL ISSUE *Enantioseparation*

Enantioseparation of fluorinated 3-(aryl)thio-4,4'-bipyridines: insights into chalcogen and π-hole bonds in high-performance liquid chromatography

Paola Peluso,[a,*] Carlo Gatti,[b,c] Alessandro Dessì,[a] Roberto Dallocchio,[a] Robin Weiss,[d] Emmanuel Aubert,[e] Patrick Pale,[d] Sergio Cossu[f] and Victor Mamane[d,*]

[a] Istituto di Chimica Biomolecolare ICB, CNR, Sede secondaria di Sassari, Traversa La Crucca 3, Regione Baldinca, 07100 Li Punti - Sassari, Italy

[b] CNR-ISTM, Istituto di Scienze e Tecnologie Molecolari, via C. Golgi 19, 20133 Milano, Italy

[c] Istituto Lombardo Accademia di Scienze e Lettere, via Brera 28, 20121 Milano

[d] Institut de Chimie de Strasbourg, UMR CNR 7177, Equipe LASYROC, 1 rue Blaise Pascal, 67008 Strasbourg Cedex, France

[e] Cristallographie, Résonance Magnétique et Modélisations (CRM2), UMR CNRS 7036, Université de Lorraine, Bd des Aiguillettes, 54506 Vandoeuvre-les-Nancy, France

[f] Dipartimento di Scienze Molecolari e Nanosistemi DSMN, Università Ca' Foscari di Venezia, Via Torino 155, 30172 Mestre Venezia, Italy

* Corresponding author. E-mail address: p.peluso@icb.cnr.it. Tel.: +39 079 2841218.

* Additional corresponding author. E-mail address: vmamane@unistra.fr. Tel.: +33 368 851612.

ABSTRACT

A chalcogen bond (ChB) is a σ-hole-based noncovalent interaction between a Lewis base and an electrophilic element of Group VI (O, S, Se, Te), which behaves as a Lewis acid. Recently, we demonstrated that halogen bond, the more familiar σ-hole-based interaction, is able to promote the enantioseparation of chiral compounds in HPLC environment. On this basis, an investigation to detect ChBs, functioning as stereoselective secondary interactions for HPLC enantioseparations, was started off and the results of this study are described herein. Our investigation also focused on the impact of the perfluorinated aromatic ring as a π-hole donor recognition site. For these purposes, seven atropisomeric fluorinated 3-arylthio-4,4'-bipyridines were designed, synthesized and used as potential ChB donors (ChBDs) with two cellulose-based chiral stationary phases (CSPs) containing carbonyl groups as ChB

acceptors (ChBAs). In addition, one and two analogues lacking fluorine and sulphur, respectively, were prepared as terms of comparison. The design of the test analytes was computationally guided. In this regard, electrostatic potentials (EPs) associated with σ- and π-holes were computed and the atomic contributions to the sulphur EP maxima were derived using a molecular space partitioning in terms of Bader's atomic basins. This procedure is akin to the Bader-Gatti electron density source function (SF) decomposition, yet suitably extended to the EP field. For five 3-substituted-4,4'-bipyridines, thermodynamic parameters were derived from van't Hoff plots. Finally, the use of molecular dynamic (MD) simulation to model ChB in cellulose-analyte complexes was explored. Evidences that σ-hole and π-hole interactions can jointly drive HPLC enantioseparations through recognition sites generated by electronic charge depletion emerged from both experimental results and theoretical data.

Keywords: Bipyridines; Chalcogen bond; Electrostatic potential surfaces; Molecular dynamic; Polysaccharide-based chiral stationary phases; Source function

1. Introduction

The enantioseparation of chiral compounds through the so-called direct approach is an important matter in several fields of chemistry, biochemistry and life science [1,2]. The direct approach is based on the formation of transient diastereomeric selectand-selector complexes in a chiral environment generated by a chiral selector. Although the corresponding basis is conceptually simple, understanding the recognition pattern occurring in these processes remains a demanding issue in separation science [3]. Indeed, along with strong long-range interactions involved in the non-stereoselective binding, diverse short-range directional interactions based on the complementarity of selector and analyte (electrostatic fit), including hydrogen bonds, π-π, dipole–dipole, and van der Waals interactions [4], are able to promote the enantioseparation. Moreover, steric and hydrophobic factors can also play a role [1,5].

More recently, σ-hole bonds involving atoms of Groups IV–VII have also been considered as important directional noncovalent interactions [6,7]. A σ-hole indicates the region of positive electrostatic potential (EP) found on an anti-bonding σ* orbital, located along the elongation of the corresponding covalent bond. Typically, a σ-hole bond, written as EWG-$D_\sigma\cdots A$ (B_L), results from the interaction of a donor atom D_σ, acting as a Lewis acid, with an acceptor A behaving as a Lewis base (B_L). The electron-withdrawing group (EWG) covalently attached to D_σ redistributes the electron density on D_σ itself (anisotropy), forming electron-deficient σ-holes which, consequently, act as a Lewis acid. In general, the depth of a σ-hole increases as the polarizability of D_σ [8].

The most common and well known of these σ-hole bonds are halogen bonds (XB), involving a halogen atom and various Lewis bases (Fig 1A) [9]. Besides XBs, σ-hole interactions involving chalcogen atoms have also been identified, leading to the so-called chalcogen bonds (ChBs). Although less studied than XBs, recent years have witnessed some applications in materials and crystal engineering [10], self-assembly processes [11], anion binding and transportation [12,13], and catalysis [14,15].

Analogously to the XB, ChB results from interaction between an electrophilic chalcogen (Ch) atom (Group VI: O, S, Se, Te) and a donor B_L (Fig. 1B). As XB, the main characteristics of ChB are directionality and tunability. Due to Ch valency, two regions of positive EP are localized on the outer part of the Ch atom, opposite to each EWG (typical EWG–Ch···B_L bond angles are close to 180°), and the strength of the ChB can be tuned by varying Ch atom, EWG and B_L [10].

Conceptually analogous to the σ-hole bond, a π-hole bond is a noncovalent interaction which involves an unpopulated π* orbital (π-hole), as a donor, and a B_L as acceptor (anion or lone-pair). A typical π-hole is located perpendicular to the molecular framework of perfluorinated aromatic rings (Fig. 1C) [6,16].

Recently, our groups discovered that XBs can drive HPLC enantioseparations of halogenated analytes (XB donors) [17] by using cellulose tris(3,5-dimethylphenylcarbamate) (CDMPC) as a chiral selector (XB acceptor) [18,19], enlarging the range of interactions which are active in HPLC environment (Fig. 2). Later, envisaging for the polysaccharide derivatives a novel function other than resolution of racemic mixture [20], we showed that HPLC and polysaccharide-based chiral stationary phases (CSPs) could be used as technical and molecular tools, respectively, for the detection of stereoselective XBs [21].

We describe herein our investigations aiming to detect, in HPLC environment, other interactions involving regions of electronic charge depletion as recognition sites at both chiral and achiral level. For this purpose, atropisomeric 4,4'-bipyridines **1**, **2** and **5**-**10** (Fig. 3) were designed as potential ChB donors (ChBDs). In addition, compounds **3** and **4**, lacking sulphur at position 3, were studied with the aim to evaluate the impact of the pentafluorophenyl-centred π-hole on the enantioseparation.

For all compounds, EPs were computed [22], and atomic contributions to the EPs maxima of sulphur in **1**-**5**, associated to ChBs, were derived using a molecular space partitioning in terms of Bader's atomic basins [23]. This procedure is akin to the Bader-Gatti electron density source function (SF) approach [24-26], suitably extended to the EP field [27,28].

It is worth mentioning that studies on both stereoselective ChB and π-hole bonds are unprecedented. Furthermore, currently, S···O=C contacts have attracted interest because they have proved to control protein folding and likely regulate enzymatic functions [6].

2. Experimental

2.1. Chemicals

The syntheses of compounds **1**-**10** together with their names and ^{1}H and ^{13}C NMR and HRMS spectra are available in the Supplementary data.

2.2. Chromatography

An Agilent Technologies (Waldbronn, Germany) 1100 Series HPLC system (high-pressure binary gradient system equipped with a diode-array detector operating at multiple wavelengths (220, 254, 280, 360 nm), a programmable autosampler with a 20 μl loop, and a thermostatted column compartment) was employed for both analytical and multimilligram separations. Data acquisition and analyses were carried out with Agilent Technologies ChemStation Version B.04.03 chromatographic data software. The UV absorbance is reported as milliabsorbance units (mAU). Lux Cellulose-1 (Phenomenex, USA), Chiralcel OD (Daicel, Tokyo, Japan) (cellulose tris(3,5-dimethylphenylcarbamate); 10 μm), Lux Cellulose-2 (cellulose tris(3-chloro-4-methylphenylcarbamate); 5 μm, Phenomenex), Chiralpak IC (cellulose tris(3,5-dichlorophenylcarbamate); 5 μm) and Chiralpak IA (amylose tris(3,5-dimethylphenylcarbamate); 5 μm) (Chiral Technologies Europe, Illkirch, France) were used as chiral columns (250 × 4.6 mm). HPLC grade ethanol (EtOH), *n*-hexane (Hex), *n*-heptane, methanol (MeOH), and 2-propanol (IPA), were purchased from Sigma-Aldrich (Taufkirchen, Germany). The retention factor (k) was determined as $k = (t_R\text{-}t_0)/t_0$, where t_R is the retention time for the eluted enantiomer. Dead time (t_0) was measured by injection of tris-*tert*-butylbenzene (Sigma-Aldrich) as a non-retained compound [29]. Analyses were performed in isocratic mode at 25°C. The flow rate (*FR*) was set at 0.8

ml/min for analytical separations. For compounds **1**, **2** and **4**, the enantiomer elution order (EEO) was determined by injecting enantiomers of known absolute configuration. The absolute configuration was assigned as reported in the Supplementary data. The van't Hoff experiments were conducted at 10, 15, 20, 25, 30 and 35°C in a thermostatted column chamber equipped with a cooling system. When the temperature was changed, the column was allowed to equilibrate for 1 h before injecting the samples. Additional details on determination of thermodynamic parameters are reported in Supplementary data.

2.3. Computational studies

Conformational search was performed through molecular mechanics, using the MMFF94 force field and the Spartan '10 Version 1.1.0 (Wavefunction Inc., Irvine, CA) program [30]. Geometry optimization and computation of electrostatic potentials surfaces (EPSs) and related parameters (EP extrema, maxima and minima values, given in kJ/mol) were performed and graphically generated (Spartan '10 Version 1.1.0) employing the density functional theory (DFT) method with the B3LYP functional and the 6-311G* basis set (available for elements H-Ca and Ga-Kr). Calculated EPs for 4,4'-bipyridines **1**-**10** are available in the Supplementary data. Values of the electrostatic potential onto an isovalue electron density surface were used as an indicator of the anisotropy of the molecular charge distribution. The surface mapped values of EP as derived from Spartan '10, used the default values of the program (electron density isovalue 0.002 au, high resolution). EPS colours towards red depict negative mapped potentials, while colours towards blue depict positive potentials and colours in between (orange, yellow, green) depict intermediate values of the mapped potential. Min EP and max EP are the local minimum(a) and the maximum(a) values of the mapped property. Search for the exact location of such EP extrema was made through the Multiwfn code [31] and through its module enabling quantitative analyses of molecular surfaces [32] for several isovalue surface fields and mapped properties thereon.

Experimental details for SF calculations and MD are available in the Supplementary data. Source contribution analysis results for compounds **1**, **2** and **5**-**7** are reported in the Supplementary data_Appendix.

3. Results and discussion

*3.1. Design and syntheses of analytes **1** and **2** with properties as chalcogen bond donors*

The design of new compounds serving as ChBDs was based on structural and electronic engineering on the electron-poor 4,4'-bipyridine core. In order to obtain analytes whose chromatographic response was dependent on the σ-hole depth of sulphur, we envisaged tuning the chiral 4,4'-bipyridine core **11** (Fig. 4), in which two bromines and one sulphur close to the stereogenic axis serve as atropisomerism inductors and potential Ch site, respectively. The electronic adjustment of sulphur could be achieved in principle through either i) activation with chlorines leading to compound **1**, or/and ii) phenyl perfluorination, such as in **2**.

3.1.1 Electrostatic potentials and their source contribution at the sulphur electrostatic potential maxima

To prove the efficacy of the double activation engineered on **11**, EPSs of these compounds were generated by mapping EP onto electron density isosurfaces (Supplementary data). The EP analysis is widely used for exploring and studying noncovalent interactions [33,34].

The distribution of the mapped EPs showed two sulphur-centred σ-holes, σ_1 and σ_2, as two narrow separated positive regions which surround the most electron-poor sites corresponding to the max EP values on sulphur. These regions are located along the elongation of each C-S bond (Fig. 4), σ_1 (at the top of Het-S bond, Het = $C_{10}H_5Br_2N_2$ for **11**, and $C_{10}H_3Br_2Cl_2N_2$ for **1** and **2**) being more electronically activated and sterically accessible than σ_2 (at the top of S-Ar bond, Ar = C_6H_5 for **11** and **1**, and C_6F_5 for **2**) (Table 1). Indeed, in compound **2** the max EP associated to σ_1 increases (+115%) more than the max EP of σ_2 (+38.3%), relative to the corresponding EP values in **11**.

From this EP analysis, different effects on σ_1 and σ_2 can be assigned to the two types of activation: i) the introduction of two chlorines, at positions 2 and 2' (compound **1**), increases the max EP value of σ_2 (+ 39.6%) more than for σ_1 (+ 12.6%); ii) on the contrary, upon subsequent perfluorination (compound

2), the max EP value of σ_1 increases dramatically (+ 91%), whereas the max EP in σ_2 remains almost unchanged.

In addition, in compound **2**, a positive EP on the perfluorinated aromatic ring revealed the presence of a π-hole as a potential recognition site. Moreover, in **1** and **2** the common 5,5'-dibromo-2,2'-dichloro-4,4'-bipyridyl scaffold showed four halogen-centred σ-holes.

With the aim to examine in depth the origin of the EP on sulphur, we applied the SF [24] EP decomposition [27,28] to the sulphur-centred σ-holes in both **1** and **2**. Within this approach, each EP value may be envisaged as due to source contributions from atoms or groups of atoms of a system. On this basis, it is possible to evaluate how the EP at the σ-hole is influenced by the remaining parts of the system and the small or large extent of such influence is just quantified by the SF. In Table 2, the EP SF decomposition in **1** and **2** at the EP maxima of sulphur σ_1 and σ_2 is reported. The values of V represent the SF contributions of the listed atomic groups, while those of ΔV express the change of such contributions on passing from **1** to **2** [ΔV = V(**2**) - V(**1**)]. The sign of source is positive or negative whether the atomic (or group) source concurs or opposes to the positive potential of σ_1 and σ_2.

In Table 2, the sum of V(Het)+V{All [C_{Ar} + H_{Ar} (or F)$_{Ar}$]}+V(S) reproduces, as expected, the observed EP maxima in **1** and **2**. The V(Het) contributions include those of the halogen atoms, which are also separately listed. The latter remain almost constant, on passing from **1** to **2**, for both σ_1 and σ_2 maxima (ΔV(Het) = 0.0004 and -0.0018 au, respectively), while V(Het) similarly increase for both maxima in **2** (ΔV(Het) = 0.0060 and 0.0057 au, respectively). What leads to a much larger σ_1 maximum upon fluorination is the almost doubling of the S atom contribution, from 0.0359 (**1**) to 0.0665 au (**2**). For σ_1, the ΔV(S) (0.0306 au) largely overwhelms the negative contribution of the [C_{Ar} + F_{Ar}] group (ΔV = -0.0162 au), while for the σ_2 maximum the opposite occurs (ΔV(S) = 0.0099 au; ΔV(All [C_{Ar} + F_{Ar}]) = -0.0157 au), due to the different geometrical location of the two maxima. Due to the large electron-withdrawing power of fluorine, the sulphur atom becomes more positively charged upon

fluorination (q(S) = 0.122 and 0.208 e^-, where q(S) is the Bader's net charge in **1** and **2**, respectively), hence more able to produce positive EP regions in **2**, relative to **1**. However, such an effect is three times as big at the top of Het-S bond (σ_1) than at the top of S-Ar bond (σ_2), [ΔV(S) = 0.0306 and 0.0099 au], owing to the much closer proximity of the former to the strong electron-withdrawing F atoms. The presence of F atoms makes the C_{Ar} atoms highly electropositive (Δq(C) about 0.5 e^-), the sulphur more positively charged and polarized in a direction counter to C-F and S-F charge transfer. Fluorination of the aryl ring has therefore a large enhancement effect on the σ_1 hole of sulphur due to the induced large EP contribution increase from sulphur, although the presence of F atoms renders V(C_{Ar} + F) highly negative, relative to V(C_{Ar} + H) and even more so for σ_1. In addition, geometrical parameters for the two maxima on sulphur were derived from calculations (**1**, σ_1: 1.91 Å, Het-S-σ angle 170.79°; σ_2: 1.94 Å, Ar-S-σ angle 164.30°) (**2**, σ_1: 1.94 Å, Het-S-σ angle 165.04°; σ_2: 2.02 Å, Ar-S-σ angle 154.50°).

*3.1.2 Syntheses of 3-arylthio-4,4'-bipyridines **1** and **2***

In practice, racemic **1** and **2** were prepared by reaction of the *in situ* generated lithio intermediate **12** with 1,2-diphenyldisulfide and 1,2-bis(pentafluorophenyl)disulfide, respectively. The intermediate **12** was prepared by iodine – lithium exchange performed starting from 4,4'-bipyridine **13** (Scheme 1) [35].

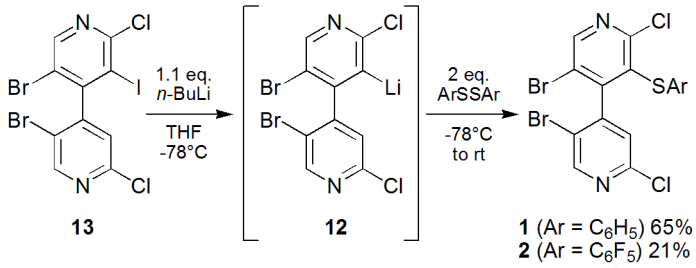

Scheme 1. Synthesis of 4,4'-bipyridines **1** and **2**.

Under these conditions, **1** and **2** were obtained with 65% and 21% yield, respectively (see Supplementary data for details), and enantioseparated by HPLC. Assignment of absolute configuration for **1** was achieved by single crystal XRD analysis, whereas for **2**, ECD spectroscopy coupled with TD-DFT calculations was used because it could not be crystallized (Supplementary data).

3.2. Comparative enantioseparation of 3-phenylthio- and 3-pentafluorophenylthio-4,4'-bipyridine

The chromatographic behaviour of compounds **1** and **2** was evaluated expecting responses being strictly dependent on the electronic features of the distinctive substituent at position 3 [18]. Four chromatographic systems were generated by the combination of CDMPC with either Hex/IPA 90:10 (*mix A*), hex/IPA/MeOH 90:5:5 (*mix* B) or MeOH 100% (*mix C*) and cellulose tris(3-chloro-4-methylphenylcarbamate) (CCMPC) with *mix A*: CDMPC/*mix A*, CCMPC/*mix A*, CDMPC/*mix B* and CDMPC/*mix C*. These four systems were used in parallel, as an orthogonal HPLC protocol [21].

In the polysaccharide-based CSPs the glucosyl backbone determines conformational chirality [36], whereas the derivatization of the native polymer allows a perpendicular molecular expansion (with respect to the backbone axis) and the transfer of the chiral information to generate a chiral polymeric groove which is able to host and recognize enantiomers. In this context, a polar layer containing carbonyl oxygens is located inside the polymer groove, whereas a hydrophobic layer containing substituted aromatic rings is located outside the polymer groove [37]. The presence of methyl, as electron donating group, or chlorine, as EWG, on the aromatic ring influences the capability of the carbonyl oxygens as Lewis bases [20] and, consequently, their properties as σ- / π-hole acceptors. On this basis, in CDMPC the carbonyl oxygens show enhanced properties as acceptors (min EPc$\underline{o}$ = -170 kJ/mol), while the CCMPC carbonyls exhibit reduced acceptor capability induced by EW chlorine substituents (min EPc$\underline{o}$ = -158 kJ/mol) [38]. Moreover, the properties of the carbonyl oxygens can be triggered by tuning the MP. Indeed, hex/IPA-containing normal phase (NP) elution conditions (such as *mix A*) have proved to assist interactions involving the polar layer. On the contrary, MeOH-containing MPs (*mix B* and *C*) were found to destabilize σ-hole bonds forming hydrogen bonds with the polar layer and promoting hydrophobic contacts [19,20].

On this basis, the orthogonal HPLC protocol was applied to **1** and **2** (Table 3). Retention was shown to be slightly affected by the orthogonal conditions and, indeed, k_1 values for the first eluted (*M*)-enantiomers range from 1.01 to 1.14 and from 0.87 to 1.26 for **1** and **2**, respectively. Analogously, both k_2 and α values of **1** were scarcely influenced by any change of the chromatographic system (CSP and/or MP) (entries 1-4). In these cases, hydrophobic forces seemed to control retention and selectivity. On the contrary, a different behaviour was observed for compound **2** because k_2 for the second eluted (*P*)-enantiomer and α values seemed to be deeply influenced by changes of analyte and CSP structures as well as MP polarity (entries 5-8). On this basis, a thorough comparative analysis of chromatographic data, computed electronic properties and thermodynamic parameters, derived from van't Hoff plots, suggested that a stereoselective secondary interaction, strictly dependent on the pentafluorophenylthio substituent at the position 3 of the 4,4'-bipyridine scaffold and involving the carbamate carbonyl oxygen of the CDMPC, could explain the diverse separation outcomes of **2** and **1**. In fact, taking into account the effect of focused changes of donor/acceptor structures and MP, the following observations emerged:

i) e*ffect of changing analyte structure (entries 1 and 5)*. As changing the group at the 3-position induced different separation outcomes for **2** and **1**, this effect could be correlated to σ_1-hole depth. Indeed, the distinctive pentafluorophenylthio group in **2** generates a more electrophilic σ_1 than the (phenyl)thio group in **1**, giving, therefore, a possible explanation for the different behaviour of the two (*P*)-enantiomers, with a 79.5% decrease in the k_2 value of **1** compared to **2**, under identical elution conditions (CDMPC/*mix A*). In addition, as **2** exhibits a distinctive π-hole, the latter could act as a recognition site, impacting the enantioseparation extent, through a π-hole interaction involving CSP carbonyl oxygen as B_L (Fig. 1C). On the other hand, in this compound the two chlorine-centred σ-holes at positions 2,2' showed low depth and scarce capability to control selectivity [19,38]. Analogously, our previous studies on XB-driven enantioseparations had showed that 5,5'-bromine-centred σ-holes, with max EP = 123.3 kJ/mol, are only able to produce moderate selectivity (α = 1.47) [19];

ii) e*ffect of changing polysaccharide structure (entries 1 vs 2 and 5 vs 6)*. By changing CDMPC to CCMPC, the separation factor of **2** dramatically dropped with a 75.2% decrease, whereas the separation factor of **1** showed a decrease of just 3.4%. This behaviour could be related to the reduced Lewis basicity of the carbonyl groups of the CCMPC;

iii) e*ffect of changing medium polarity (entries 1 vs 3-4 and 5 vs 7-8)*. On CDMPC, the addition of MeOH (*mix B* and *mix C*) enhanced MP polarity and introduced in the chromatographic system a competitive electrophile. Consequently, selectivity decreased for **1** and **2** of 2.6% and 31.3% with *mix B* and of 13.8% and 61.4% with *mix C*, respectively;

iv) *analysis of thermodynamic parameters (Table 4)*. As both retention and separation are influenced by temperature, a variable temperature study was carried out between 10 and 35°C for 4,4'-bipyridines **1** and **2** on the four chromatographic systems. Because the van't Hoff plots were linear in the considered temperature range ($r^2 \geq 0.9958$) (Supplementary data), enthalpy and entropy values derived from the plots allowed to evaluate the enthalpic and entropic contribution to enantioseparations. The derived thermodynamic parameters showed that the enantiomeric separation of **1** and **2** are enthalpically driven ($\Delta\Delta H < 0$ and $\Delta\Delta H < T\Delta\Delta S$) under all elution conditions. Negative ΔS indicated an increase in the order of the chromatographic system as the solute moved from mobile phase to stationary phase. In particular, with the system CDMPC/*mix A*, the second eluted enantiomer (*P*)-**2** showed values of enthalpy, entropy and free energy much lower than those of (*P*)-**1**, confirming the pivotal role of the $-SC_6F_5$ group to exert polar interactions with the CSP. It is worth mentioning that, under the same elution conditions (CDMPC/*mix A*), the thermodynamic behaviour of the couple **1**/**2** seemed to follow the same trend of the compounds 2,2',3,3',5,5'-hexachloro- (**14**) / 2,2',3,3',5,5'-hexaiodio-4,4'-bipyridine (**15**) [21] which differ in the capability to exert σ-hole interactions in HPLC environment, iodine being privileged σ-hole donor. Indeed, $\Delta\Delta H$, $\Delta\Delta S$ and $\Delta\Delta G$ values associated to **1** are very similar to the values of the poor σ-hole bond donor **14** ($\Delta\Delta H$ = -1.95 kJ·mol^{-1}, $\Delta\Delta S$ = -5.36 J·K^{-1}·mol^{-1} and $\Delta\Delta G$ = -0.35 kJ·mol^{-1}), whereas **2**

was characterized by higher entropic stabilization as it occurs with the good σ-hole donor **15** [ΔΔS = -27.47 $J \cdot K^{-1} \cdot mol^{-1}$] [21].

On the other hand, the values of the thermodynamic parameters, obtained for **1** and **2** with the chromatographic system CDMPC/*mix C*, proved the higher recognition ability of the selector toward the enantiomers of **2** compared to **1**. In addition, this behaviour under polar organic (PO) elution conditions could be due to higher hydrophobicity and more efficient π-π stacking of **2** with respect to **1** (Log $P_{\text{partition coefficient}}$: 6.09 (**1**) < 6.88 (**2**)).

*3.3. Enantioseparation behaviour of compounds **5-10**: effect of the position and number of fluorine atoms*

Having identified the main features of the chromatographic behaviour of **1** and **2**, the enantioseparation of compounds **5-10** was explored with the aim to evaluate the effect of diverse fluorine substitution patterns on the enantioseparation, looking at the role the position (compounds **5-7**) and number (compounds **8**, **9** and **10**) of fluorine atoms could have. All these compounds were prepared by iodine – lithium exchange performed on 4,4'-bipyridine **13** and subsequent electrophilic trapping of the lithio intermediate **12** with the proper disulphide (30-71% yields), as reported in Scheme 1 for **1** and **2** [35].

In Table 5, retention and selectivity factors observed for compounds **5-10** with the chromatographic system CDMPC/*mix A* are reported (entries 2-7) along with the corresponding parameters of **1**, as a term of comparison (entry 1).

For the mono substituted series **5-7** (entries 2-4), containing a single fluorine atom at the 3-possible positions of the phenyl group (*ortho*, *meta*, *para*), retention was only slightly affected by the substitution pattern and, indeed, k_1 values for the first eluted enantiomers range from 1.20 to 1.22. Analogously, both k_2 and α values of **5-7** were scarcely influenced by any change of fluorine position, nevertheless

selectivity was shown to decrease following the order *o*-F > *m*-F > *p*-F (Fig. S7). For these compounds, a clear correlation between max EP on σ_1, max EP on Ar_F and k_2 or α was not observed. In particular, no positive value of EP related to π-hole was found for **5** and **6**, whereas a slight depletion of the electron density characterizes **7**.

With the aim to examine in depth the effect of fluorine pattern on σ_1 EP, the SF descriptor was applied to the sulphur σ-holes (σ_1) in **5**-**7**. The results of calculations are illustrated in Table 6. Each σ_1 EP value may be expressed as a sum of contributions from the S and F atoms and from the Het and $(C+H)_{Ar}$ groups. Data in Table 6 reveal that the single F substitution largely decreases the SF contribution of the S atom to σ_1, from 0.0665 au in **2** (Table 2) to an average value of only 0.0388 au in **5**-**7**, slightly larger than for the unsubstituted compound **1** (0.0359 au). Indeed the average (**5**-**7**) net positive charge of sulphur is 0.139 e^-, much closer to that found in **1** (0.122) than in **2** (0.208). Increase of the sulphur positive charge upon fluorination follows the substitution pattern, being larger when the fluorine is closer and smaller when it is further from S (0.152, 0.140 and 0125 for *ortho*, *meta* and *para* F-substitution). Thus, the highest V(S) contribution turns out to be that of the *ortho*-F compound **5**. The V(S) contribution for the *para*-F compound is, instead, surprisingly similar and even slightly larger than that of the *meta*-F compound. This becomes no longer a surprise when it is realized that the σ_1-hole is indeed slightly closer to the F nucleus in **7** than in **6** (5.44 and 5.70 Å, respectively), because *meta*-F substitution leads to a *trans* rather than to a *cis* σ_1-S-C_{Ar}-F minimum geometrical conformation. As a result, the negative V(F) contribution, counteracting the positive V(S) contribution, is lowest in magnitude for the *meta*-F compound. The sum of V(F) and V(S) contributions already accounts for the σ_1 trend in **6**-**7** compounds (-0.0236 and -0.0249 au, respectively). Despite the more negative V(S+F) contribution in **5** relative to **7** (-0.0416 and -0.0249 au, respectively), almost equal σ_1 values occur for *ortho* (**5**) and *para* (**7**) F-substitution. This arises because of a larger positive contribution of the C atom linked to the fluorine (these contributions are denoted in bold in Table 6) which compensates the more

negative V(S+F) contribution (-0.0416 and -0.0249 au, respectively). The small changes in the V(Het) values play only a minor role in defining the σ_1 trend in **5-7** compounds. The SF analysis of the σ-holes in **5-7** allows for an unprecedented insight on the effect of the F-substitution pattern. Minimum energy geometrical conformation also plays a significant role and it cannot be ignored. If not taken into account, the largest σ_1 value for **6** could not find an easy explanation. The largest F distance from σ_1 in the *meta* substituted compound realizes the best compromise between the activation of S induced by the presence of the F atom and the counteracting effect on the EP positive σ-hole due to the negative EP contribution from this same atom.

This kind of analysis confirmed the pivotal role of sulphur in the enantioseparation and, in this perspective, the decrease of selectivity changing the 2,6-difluoro pattern of **8** (Table 5, entry 5, $\alpha = 1.18$) to the 2,4-difluoro of **9** (Table 5, entry 6, $\alpha = 1.11$) could be explained on the basis of the minor overall contribution to σ_1 induced by the second fluorine located at the *para* position compared to the *ortho* position.

Concerning the effect induced by the number of fluorine atoms on the aromatic ring, in the series **5**, **8** and **10** (Table 5, entries 2, 5 and 7) respectively containing 1, 2, and 3 fluorine atoms, respectively, k_1, k_2 and α increased as the number of fluorine atoms (Fig. S8) and, in particular, selectivity tended to increase moderately as the max EP on σ_1 and Ar_F. Accordingly, thermodynamic parameters derived for compound **8** (Table S7) are lower than the corresponding values associated to the enantioseparation of **1**, under the same elution conditions (CDMPC/*mix A*).

3.4. Impact of recognition sites generated by electronic charge depletion: σ-hole vs π-hole.

Finally, with the aim to distinguish the contribution of the chalcogen site (sulphur) from that of the fluorinated π-hole, compounds **3** and **4** were designed and prepared by deprotolithiation of 2,2'-dichloro-5,5'-dibromo-4,4'-bipyridine **16** [35] (Scheme 2). Then, lithio intermediate **12** was trapped by the proper electrophile (pentafluorobenzyl bromide or hexafluorobenzene), furnishing **3** and **4** (18% and

353 5% yields, respectively). Assignment of absolute configuration for **4** was achieved by single crystal
354 XRD analysis (Supplementary data).

355 The orthogonal HPLC protocol was applied to compounds **3** and **4** and the obtained chromatographic
356 results were compared to the corresponding outcomes of **2** (Table 7).

357 The comparison between the chromatographic profiles (Fig. S9) and parameters of compound **2**, **3**
358 and **4** proved the pivotal role of the π-hole on the perfluorinated phenyl ring as recognition site. Indeed,
359 the following observations emerged:

360 i) in general, compound **4** showed lower retention and selectivity compared to **2** and **3** and a different
361 recognition mechanism seemed to occur. From the EPS generated for **4** by calculation, it could be
362 observed that the aromatic ring at the position 3 of the 4,4'-bipyridine scaffold is sterically hindered by
363 the adjacent chlorine at the 2 position. This condition prevents the penetration of the analyte into the
364 groove as proved by the low values of retention of both first and second eluted peaks obtained for **4** with
365 all four chromatographic systems. This hypothesis appeared in agreement with the positive values of
366 $\Delta G_{298\ K}$ derived for **4** in almost all cases (Table S8), depending on the lower value of the entropic term
367 $T\Delta S$ compared to the enthalpic term ΔH in the Gibbs equation ($\Delta G = \Delta H - T\Delta S$, $\Delta H < 0$ and $T\Delta S <$
368 ΔH). On this basis, weak hydrophobic π-π interactions between the analyte and the aromatic moieties in
369 the outer regions of the CSP are likely to govern selectivity in this case. Indeed, by introducing MeOH
370 in the MP (*mix B*), which favours hydrophobic behaviours, selectivity of **4** on CDMPC increases
371 compared to the selectivity obtained with *mix A* on the same CSP.

372 ii) it is worth comparing the chromatographic behaviours of the couple 5,5'-dibromo-2,2'-dichloro-3-
373 phenyl-4,4'-bipyridine (**17**) / **1** (Fig. S10) and the couple **4** / **2** (Fig. S9). In both cases, the substitution
374 pattern of **17**, **4** and **1**, **2** can be correlated by introducing a sulphur atom as spacer between the
375 heteroaromatic scaffold and the phenyl ring. Interestingly, this structural variation has a dramatic effect

on selectivity only for **2**, which bears both σ- and π-hole, whereas it has no effect for **1**. Indeed, the enantioseparation traces of **1** and **17** are superimposable (Fig. S10);

iii) the EPS generated for compound **3** showed a more accessible π-hole due to the presence of a methylene (-CH_2-) spacer between the 4,4'-bipyridine and the perfluorinated ring, even with a lower depth (89.9 kJ/mol) compared to **4** (101.1 kJ/mol). For **3**, higher retention and selectivity were observed compared to **4**, which are likely due to the conformational flexibility induced by the methylene spacer. In particular, on CDMPC, **3** showed lower values of ΔΔH compared to **4**. On the contrary, on CCMPC higher values of ΔΔH and ΔΔS were derived for **3**. These variations dependent on the CSP structures appeared consistent with a mechanism controlled by a lone pair-π-hole bond, involving **3** and the carbonyl lone pair in the inner part of the CSP. In this perspective, as the Lewis basicity of the carbonyl decreases in the CCMPC, consequently, enantiomer thermodynamic stabilization also decreases. On the contrary, for **4** the thermodynamic stabilization by means of π-π interactions is higher with the distinctive 3-chloro-4-methylphenyl (CCMPC) compared to the 3,5-dimethylphenyl (CDMPC), likely because of different stereoelectronic properties;

iv) compound **2** showed higher k_2 and selectivity than **3** on CDMPC, whereas lower retention and selectivity on CCMPC were observed. On the contrary, the two compounds showed very similar selectivity on CDMPC with *mix C*, where pure MeOH, as MP, prevent formation of polar interactions. Taking into account that the substitution pattern of **3** and **2** could be correlated by changing the methylene spacer to sulphur at the 3-position, the critical function of sulphur on selectivity emerged.

Analysis of the collected thermodynamic parameters for **1**-**4** and **8** (Tables 4, S7 and S8) revealed that ΔΔH and ΔΔS change proportionally. The changes in the two quantities essentially cancel out each other, resulting in only small changes in ΔΔG. This phenomenon is known as entropy-enthalpy compensation (EEC) and is illustrated graphically by the linear relationship between ΔΔH and ΔΔS (Fig. 5A). Enthalpy-entropy compensation gave a straight line with a good correlation coefficient (r^2= 0.9954)

and no deviation from linearity was observed. This could confirm that the same type of discrimination mechanism governs the examined enantioseparations with a level of efficacy dependent on the substitution pattern.

With the aim to examine in depth the results of the EEC, the residual ($\Delta\Delta S_{predicted} - \Delta\Delta S_{experimental}$) plot values (Table S9) derived from the linear regression analysis were compared (Fig. 5B). Taking the sum of the residual values of **2** as reference absolute value (1.46), interestingly, in accord with the experimental outcomes, the corresponding absolute values calculated for **1**, **3** and **4** showed a deviation from **2** following the order **2** (1.46) < **1** (1.48) < **3** (2.0) < **4** (6.58). Interestingly, a higher deviation from linearity was observed for **3** relative to **2**, showing that slightly different retentive and enantioselective factors can operate in the discrimination of the two compounds. As expected, compound **4** showed the highest deviation from linearity due to hydrophobic factors which were shown to control retention and selectivity.

Finally, the influence of the two regions of electronic charge depletion on retention of the second eluted enantiomers was verified by simple linear regression using ln k_2 and max EPs on Ar_F (π-hole) and σ_1 as dependent and independent variables, respectively. On the basis of the described chromatographic behaviour, compound **4** was excluded from the analysis. For compounds **2**, **3** and **7**-**10**, which are characterized by positive values of EPs on Ar_F, the result of fitting a simple linear regression model to describe the relationship between ln k_2 and max EPs on Ar_F is reported in Fig. 6A (r^2= 0.9645). In this case, the P-value of the considered independent variable, max EPs on Ar_F, is 0.0005 indicating a statistically significant relationship (P-value < 0.05).

Then, for compounds **1**, **2** and **5**-**10**, the correlation between ln k_2 and the max EPs on σ_1 is reported in Fig. 6B (r^2= 0.8633). The P-value of the considered independent variable, the max EPs on σ_1, is low (0.0008), showing again a statistical significant relationship (P-value < 0.05) between selectivity and the electronic charge depletion on sulphur.

On the basis of experimental results, theoretical data and statistical evaluations, it is reasonable to conclude that both σ- and π-hole bond concur to the enantioseparation outcomes of **2**. The study of structurally similar compounds showed that the strength of each interaction strictly depends on analyte and CSP structures and MP polarity. In this regard, it is interesting to mention that several recent articles reported on the interplay between σ-hole and π-hole bonds [39].

3.5. Molecular dynamics.

MD calculations were performed to simulate the interaction modes of compound **2** with the CDMPC. A massless dummy atom (MA_D) connected to sulphur was introduced manually in **2**, by using distance (1.6 Å) and charge (0.2 units of positive charge) fixed arbitrarily (see Supplementary data for details). This simulation aimed to explore the dynamic response of the molecular system polysaccharide / **2** as the sulphur is treated as an electrophile, excluding virtually the π-hole site as a competitive electrophile. On this basis, with the aim to compare qualitatively the MD outcomes under different molecular situations, the calculations were performed with and without the MA_D, and Hex solvent effects were taken into account in accord with the elution mode used in the HPLC screening.

The MD protocol proposed herein may not lead to the selector-selectand complexes with the global minimum energy, however some interesting behaviours could be observed, which confirmed the pivotal role of sulphur as a chalcogen recognition site in **2**:

i) by carrying out 10 ns MD, the trajectory plots for CDMPC and **2** showed stable interactions when the MA_D correction was applied, with narrow fluctuations over 10 ns compared to the larger fluctuations observed when MA_D correction was not applied (Fig. S30);

ii) in all simulations performed by using the MA_D correction, contacts between sulphur and the carbonyl groups of the carbamate moieties of the CSP were observed. Taking into account that the MA_D correction was introduced arbitrarily, a measure of the geometrical parameters of the contact was not performed;

iii) finally, the occupancy graphs generated from the MD trajectories for the complexes CDMPC / (*M*)-**2** (with MA_D), CDMPC / (*P*)-**2** (with MA_D), and CDMPC / (*P*)-**2** (without MA_D) were compared (Fig. S31). The occupancy analysis allowed to evaluate which regions of space were highly populated by the analyte over 10 ns MD. Interestingly, by using the MA_D, the first eluted enantiomer (*M*)-**2** showed occupancy volumes in the outer region of the CSP, whereas for the second eluted enantiomer (*P*)-**2** occupancy volumes were also generated in the inner regions of the polymer. On the contrary, the occupancy volumes for the enantiomer (*P*)-**2** were shown to move toward the outer regions of the polymer, when the MA_D correction was not applied.

4. Conclusions

The enantioseparability of fluorinated 3-arylthio-4,4'-bipyridines on CDMPC was shown to increase as the EP related to regions of electronic charge depletion on the analyte becomes increasingly positive. This observation represents the core of our study which, on the basis of theoretical data and experimental results, furnishes evidences that stereoselective chalcogen and π-hole bonds, so far unexplored in HPLC environment, can drive enantioseparations.

Computational evaluation of molecular properties allowed to design analytes suitable as probes and, in parallel, to clarify some aspects of the observed chromatographic behaviours. A new approach, based on the extension of the Source Function tool to the EP and enabling to get insights on the chemical origin of these enantioseparation "drivers", has for the first time been proposed. Finally, the introduction of a massless dummy ligand, positively charged to mimic the electron depletion on sulphur, allowed to explore the dynamic behaviour of the enantiomers of **2** on CDMPC, obtaining theoretical results qualitatively in accord with the experimental outcomes.

On this basis, enantioseparations of atropisomeric test probes containing heavier chalcogen atoms are currently under investigations.

Acknowledgements

This work has been supported by Università Ca' Foscari di Venezia, Italy (Dipartimento di Scienze Molecolari e Nanosistemi, DSMN ADIR funds). We thank the International Center Frontier Research in Chemistry (icFRC) and the Laboratory of Excellence for Complex System Chemistry (LabEx CSC). C.G. acknowledges funding from Danmarks Grundforskningsfond (award No. DNRF93). The Service Commun de Diffraction des rayons X-Université de Lorraine is thanked for providing access to crystallographic facilities. The CINES/CEA CCRT/IDRIS is thanked for allocation of computing time (project A0030807449).

Appendix A. Supplementary data

Supplementary data associated with this article can be found, in the online version, at doi:

References

[1] G.K.E. Scriba, Chiral recognition in separation science - an update, J. Chromatogr. A 1467 (2016) 56-78.

[2] H. Lorenz, A. Seidel-Morgenstern, Processes to separate enantiomers, Angew. Chem. Int. Ed. 53 (2014) 1218-1250.

[3] J.C. Lang, D.W. Armstrong, Chiral surfaces: the many faces of chiral recognition, Current Opinion in Colloid & Interface Science 32 (2017) 94-107.

[4] H.-J. Schneider, Binding mechanisms in supramolecular complexes, Angew. Chem. Int. Ed. 48 (2009) 3924-3977.

[5] M. Lämmerhofer, Chiral recognition by enantioselective liquid chromatography: mechanisms and modern chiral stationary phases, J. Chromatogr. A 1217 (2010) 814-856.

[6] A. Bauzá, T.J. Mooibroek, A. Frontera, The bright future of unconventional σ/π-hole interactions, ChemPhysChem 16 (2015) 2496-2517.

[7] L. Brammer, Halogen bonding, chalcogen bonding, pnictogen bonding, tetrel bonding: origins, current status and discussion, Faraday Discuss. 203 (2017) 485-507.

[8] P. Politzer, J.S. Murray, T. Clark, Halogen bonding and other σ-hole interactions: a perspective, Phys. Chem. Chem. Phys. 15 (2013) 11178-11588.

[9] G. Cavallo, P. Metrangolo, R. Milani, T. Pilati, A. Priimagi, G. Resnati, G. Terraneo, The halogen bond, Chem. Rev. 116 (2016) 2478-2601.

[10] K.T. Mahmudov, M.N. Kopylovich, M.F.C. Guedes da Silva, A. J. L. Pombeiro, Chalcogen bonding in synthesis, catalysis and design of materials, Dalton Trans. 46 (2017) 10121-10138.

[11] P.C. Ho, P. Szydlowski, J. Sinclair, P.J.W. Elder, J. Kübel, C. Gendy, L. Myongwon Lee, H. Jenkins, J.F. Britten, D.R. Morim, I. Vargas-Baca, Supramolecular macrocycles reversibly assembled by Te···O chalcogen bonding, Nat. Commun. 7:11299 (2016) doi: 10.1038/ncomms11299.

[12] S. Benz, M. Macchione, Q. Verolet, J. Mareda, N. Sakai, S. Matile, Anion transport with chalcogen bonds, J. Am. Chem. Soc. 138 (2016) 9093-9096.

[13] J.Y.C. Lim, I. Marques, A.L. Thompson, K.E. Christensen, V. Félix, P.D. Beer, Chalcogen bonding macrocycles and [2]rotaxanes for anion recognition, J. Am. Chem. Soc. 139 (2017) 3122-3133.

[14] S. Benz, J. López-Andarias, J. Mareda, N. Sakai, S. Matile, Catalysis with chalcogen bonds, Angew. Chem. Int. Ed. 56 (2017) 812-815.

[15] P. Wonner, L. Vogel, F. Kniep, S.M. Huber, Catalytic carbon-chlorine bond activation by selenium-based chalcogen bond donors, Chem. Eur. J. 23 (2017) 16972-16975.

[16] A. Bauzá, T.J. Mooibroek, A. Frontera, Towards design strategies for anion–π interactions in crystal engineering, CrystEngComm 18 (2016) 10-23.

[17] P. Peluso, V. Mamane, S. Cossu, Liquid chromatography enantioseparations of halogenated compounds on polysaccharide-based chiral stationary phases: role of halogen substituents in molecular recognition, Chirality 27 (2015) 667-684.

[18] P. Peluso, V. Mamane, E. Aubert, S. Cossu, Insights into the impact of shape and electronic properties on the enantioseparation of polyhalogenated 4,4'-bipyridines on polysaccharide-type selectors. Evidence for stereoselective halogen bonding interactions, J. Chromatogr. A 1345 (2014) 182-192.

[19] P. Peluso, V. Mamane, E. Aubert, A. Dessì, R. Dallocchio, A. Dore, P. Pale, S. Cossu, Insights into halogen bond driven enantioseparations, J. Chromatogr. A 1467 (2016) 228-238.

[20] B. Chankvetadze, Recent developments on polysaccharide-based chiral stationary phases for liquid-phase separation of enantiomers, J. Chromatogr. A 1269 (2012) 26-51.

[21] P. Peluso, V. Mamane, R. Dallocchio, A. Dessì, R. Villano, D. Sanna, E. Aubert, P. Pale, S. Cossu, Polysaccharide-based chiral stationary phases as halogen bond acceptors: A novel strategy for detection of stereoselective σ-hole bonds in solution, J. Sep. Sci. 41 (2018) 1247-1256.

[22] P. Peluso, S. Cossu, Comparative HPLC enantioseparation of thirty six aromatic compounds on four columns of the Lux® series. Impact of substituents, shapes and electronic properties, Chirality 25 (2013) 709-718.

[23] R.F.W. Bader, Atoms in molecules: a quantum theory, International Series of Monographs on Chemistry 22, Oxford University Press, Oxford (1990).

[24] R.F.W. Bader, C. Gatti, A Green's function for the density, Chem. Phys. Lett. 287 (1998) 233-238.

[25] C. Gatti, F. Cargnoni, L. Bertini, Chemical information from the source function, J. Comput. Chem. 24 (2003) 422-436.

[26] C. Gatti, The source function descriptor as a tool to extract chemical information from theoretical and experimental electron densities, Struct. Bond 147 (2012), 193-286.

[27] A. Volkov, P. Macchi, L.J. Farrugia, C. Gatti, P.R. Mallinson, T. Richter, T. Koritsanszky, XD2006 - a computer program for multipole refinement, topological analysis and evaluation of intermolecular energies from experimental and theoretical structure factors (2006).

[28] C. Gatti, SF-ESI codes, Milano, Italy (2018).

[29] H. Koller, K.-E. Rimböck, A. Mannschreck, High-pressure liquid chromatography on triacetylcellulose: characterization of a sorbent for the separation of enantiomers, J. Chromatogr. A 282 (1983) 89-94.

[30] Y. Shao, L.F. Molnar, Y. Jung, J. Kussmann, C. Ochsenfeld, S.T. Brown, A.T.B. Gilbert, L.V. Slipchenko, S.V. Levchenko, D.P. O'Neil, R.A. Di Stasio Jr, R.C. Lochan, T. Wang, G.J.O. Beran, N.A. Besley, J.M. Herbert, C.Y. Lin, T. Van Voorhis, S.H Chien, A. Sodt, R.P. Steele, V.A. Rassolov, P.E. Maslen, P.P. Korambath, R.D. Adamson, B. Austin, J. Baker, E.F.C. Byrd, H. Dachsel, R.J. Doerksen, A. Dreuw, B.D. Dunietz, A.D. Dutoi, T.R. Furlani, S.R. Gwaltney, A. Heyden, S. Hirata, C-P. Hsu, G. Kedziora, R.Z. Khalliulin, P. Klunzinger, A.M. Lee, M.S. Lee, W.Z. Liang, I. Lotan, N. Nair, B. Peters, E.I. Proynov, P.A. Pieniazek, Y.M. Rhee, J. Ritchie, E. Rosta, C.D. Sherrill, A.C. Simmonett, J.E. Subotnik, H.L. Woodcock III, W. Zhang, A.T. Bell, A.K. Chakraborty, D. M. Chipman, F.J. Keil, A. Warshel, W.J. Hehre, H.F. Schaefer, J. Kong, A.I. Krylov, P.M.W. Gill, M. Head-Gordon, Advances in methods and algorithms in a modern quantum chemistry program package, Phys. Chem. Chem. Phys. 8 (2006) 3172-3191.

[31] T. Lu, F. Chen, Multiwfn: A Multifunctional Wavefunction Analyzer, J.Comp. Chem. 33 (2012) 580-592.

[32] T. Lu, F. Chen, Quantitative analysis of molecular surface based on improved Marching Tetrahedra algorithm, J. Mol. Graph. Model. 38 (2012) 314-323.

[33] K.E. Riley, K.–A. Tran, P. Lane, J.S. Murray, P. Politzer, Comparative analysis of electrostatic potential maxima and minima on molecular surfaces, as determined by three methods and a variety of basis sets, J. Comput. Sci. 17 (2016) 273-284.

[34] S. Scheiner, Comparison of various means of evaluating molecular electrostatic potentials for noncovalent interactions, J. Comput. Chem. 39 (2018) 500-510.

[35] V. Mamane, E. Aubert, P. Peluso, S. Cossu, Lithiation of prochiral 2,2′-dichloro-5,5′-dibromo-4,4′-bipyridine as a tool for the synthesis of chiral polyhalogenated 4,4′-bipyridines, J. Org. Chem. 78 (2013) 7683-7689.

[36] T. Ikai, Y. Okamoto, Structure control of polysaccharide derivatives for efficient separation of enantiomers by chromatography, Chem. Rev. 109 (2009) 6077-6101.

[37] R.B. Kasat, N.-H.L. Wang, E.I. Franses, Effects of backbone and side chain on the molecular environments of chiral cavities in polysaccharide-based biopolymers, Biomacromolecules 8 (2007) 1676-1685.

[38] P. Peluso, V. Mamane, E. Aubert, S. Cossu, High performance liquid chromatography enantioseparation of atropisomeric 4,4'-bipyridines on polysaccharide-type chiral stationary phases: impact of substituents and electronic properties, J. Chromatogr. A 1251 (2012) 91-100.

[39] H. Wang, W. Wang, W.J. Jin, σ-Hole bond vs π-hole bond: a comparison based on halogen bond, Chem. Rev. 116 (2016) 5072-5104.

FIGURE CAPTIONS

Fig. 1. Description of halogen (A), chalcogen (B) and π-hole (C) bonds.

Fig. 2. Polysaccharide-based polymers as halogen bond acceptors.

Fig. 3. Structures of the 5,5'-dibromo-2,2-dichloro-3-substituted-4,4'-bipyridines **1**-**10**.

Fig. 4. Design of potential 4,4'-bipyridine-based ChBDs.

Fig. 5. A. Enthalpy-entropy (ΔΔS *vs* ΔΔH values x 10000) compensation for compounds **1**, **2**, **3**, **4** and **8** on CDMPC and CCMPC under normal phase (NP) and polar organic (PO) elution modes (*FR* 0.8 ml/min); B. Residual plot (ΔΔS values).

Fig. 6. Linear regression analysis describing the relationships between ln k_2 and the max EP Ar_F (π-hole) (A) and the max EP on σ_1 (B) for compound **1**-**3** and **5**-**10**.

Scheme 1. Synthesis of 4,4'-bipyridines **1** and **2**.

592 **Scheme 2.** Synthesis of 4,4’-bipyridines **3** and **4**.